

Aspects of Global Magnetospheric Processes*

P. Song¹ V. M. Vasyliūnas²

1(*Center for Atmospheric Research and Department of Environmental, Earth and Atmospheric Sciences, University of Massachusetts Lowell, USA*)

2(*Max-Planck-Institut für Sonnensystemforschung, 37191 Katlenburg-Lindau, Germany*)

Abstract Magnetospheric global modeling is a method to link observations from distant regions via physical laws and has long played a unique and crucial role in space physics. It, different from computer simulations, represents the highest level of abstraction of the physical understanding of the processes that cause observed phenomena. It results in various specific models. While it appears in the form of cartoons, it is based on and has to be qualitatively consistent with physical laws. With the advancement of computer simulations, clues to the connection between physical laws and observation can be perceived much more easily than as ever before. However, computer simulation results are highly dependent on the used boundary conditions and numerical methods which may or may not represent the reality, even if the initial conditions are properly set. Therefore, simulations can easily mislead the investigations. Furthermore, a simulation result needs to be examined using diagnostic tools, such as field line tracing and streamline tracing programs. There are uncertainties in these diagnostic methods. The errors can be very large in certain areas under certain conditions. For example, a small error may link two different field lines or stream lines. The interpretations of the simulation results can be misled by these errors. The knowledge of global modeling can be useful in identifying the inconsistencies in the simulations and the flaws in the theoretical interpretation from the simulations. This review-tutorial article outlines the principles of the global modeling and discusses the successes and flaws of several global models.

Keywords Global modeling, Solar wind-magnetosphere coupling, Magnetosphere-ionosphere coupling

1 Introduction

Space physics is exciting and challenging because it studies phenomena everywhere in space in various forms. A major challenge is how to connect these phenomena in order to understand them as well as their consequences. Global, in contrast to local, aspects refer to the connections between different regions in space. A phenomenon usually involves a set of observational characteristics, interpretations of observations, and correlations with other phenomena. The most important task for observationalists is to sort out the instrumental effects, limitations of measurements, and the spatial-temporal ambiguity, and to identify the phenomenon and the processes that as-

sociated with it. Knowledge of magnetospheric global modeling may help in this process, but the power of global modeling is in full display when one is trying to link phenomena occurring in distant places in space.

The phrase “global modeling” in space physics refers to a methodology to link regions or phenomena with large spatial distances. It differs from a specific “model” and from an action of “to model”. While more people discuss global modeling, far fewer people know the principles for modeling because they are seldom described in textbooks and, hence, it is not surprising that once a while models inconsistent with these principles are presented or even published.

The origin of the global modeling can be traced back to the birth of space physics. In their pioneer-

*Supported by NSF under Award NSF-ATM0518227

Received October 19, 2009; revised April 20, 2010

E-mail: Paul_song@uml.edu

ing work, Chapman and Ferraro (1931) linked the magnetic field perturbations during magnetic storms observed on the surface of the earth to what we now call the solar wind. The link was made because that the magnetic storms appear to have a period of 27 days. However, when one traces back to the Sun, there is no obvious feature that can relate a magnetic storm because (we now know) it takes 2–3 days for the solar wind to arrive at the Earth. Furthermore, the feature that relates the Earth's magnetic perturbations is what we now know as coronal holes. There is no obvious reason why these holes, dark areas on an X-ray image, should be of any significance. Even when the concept of the plasma was not well known (Tonks and Langmuir introduced the concept of "plasma" in 1929), Chapman and Ferraro argued that ions and electrons could coexist while not forming atoms. These ionized particles come out of the coronal holes, known as the *M* (standing for magnetic disturbance) regions at the time (Bartels, 1932). The gyro motion of the ions under the influence of the earth's magnetic field produces qualitatively the same effect as we now attribute to the ring current, see Figure 1. They even estimated the speed of the solar wind to be of the order of 1000 km/s, which is in the right range of the solar wind speed during Coronal Mass Ejection (CME) events, based on the time delay from the solar activities observed on the Sun to the magnetic storm observed on the Earth.

Another fascinating story of global modeling is associated with the explanation of the antisunward convection in the polar ionosphere (see Dungey,

1995). The concept of magnetic reconnection had been significantly developed in 1950s (Dungey 1950, Sweet, 1958; Parker, 1963). The difficulty was how to link the concept of reconnection with the observations made in the ionosphere, shown in Figure 2(b). For Dungey, the founding father of modern space physics, it took over ten years to make the link (Dungey, 1961). This grand leap was the birth of the modern global modeling. In the same year, Dungey (1961) and Axford and Hines (1961) proposed completely different models to explain the same observation of antisunward ionospheric convection in the

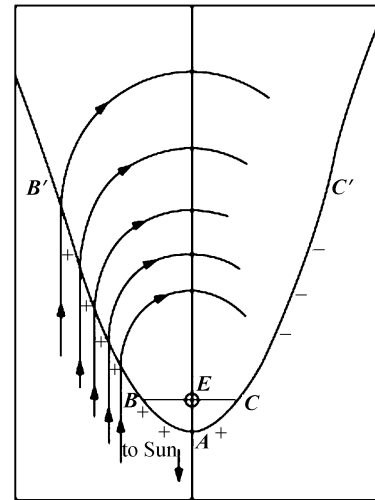


Figure 1 Solar wind stream encountering the Earth's magnetic field (Chapman and Ferraro, 1931). The gyro motions of the ions form a current by which the magnetic field induced is consistent with the magnetic field perturbations observed on the ground during magnetic storms.

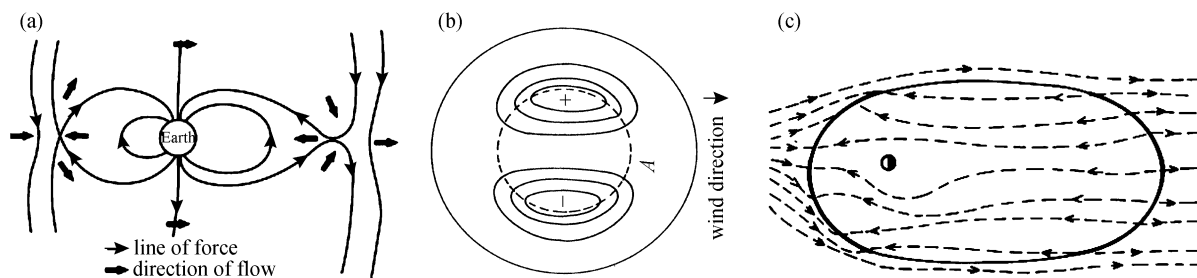


Figure 2 Solar wind-magnetosphere interaction via magnetic reconnection during southward IMF, (a) the magnetic field lines and plasma motion in the noon-midnight meridian plane (Dungey, 1961), (b) the convection in the northern polar ionosphere (Dungey, 1961), and (c) streamlines in the equatorial plane (Vasyliūnas, 1984). Thick arrowheads in (a) indicate the convection direction. The dashed circle in (b) indicates the polar cap. The solid lines in (c) show the magnetopause boundary with reconnection regions highlighted.

polar region. In Dungey’s model, see Figure 2, the plasma motion is mapped from the magnetopause to the ionosphere and become our present standard Hines (1961), on the other hand, used the viscous interaction of the solar wind flow with the magnetospheric field, see Figure 3. Note that at the time the concept of the magnetopause was not well established and the term of the magnetopause had not appeared in literature until 1964 (Hines, 1964). Nevertheless, the magnetospheric motion can be “mapped” (note the word used here) to the ionosphere and produces the same antisunward convection in either model. The principles employed in these two models are the foundations for nowadays global modeling that will be discussed in detail in this article.

The knowledge about global modeling is particularly important to computer simulationists. With the advancement of the computational capability and the numerical methods and tools, simulations can be used as an important tool for global modeling. However, simulation results are sensitive to the boundary conditions and initial conditions that are applied in a simulation, although simulationists are more focused on the numerical methods and schemes. In some instances, the numerical implementations of the resistance in the critical regions can also result in substantially different results. While the field line tracing and streamline tracing software is a very powerful

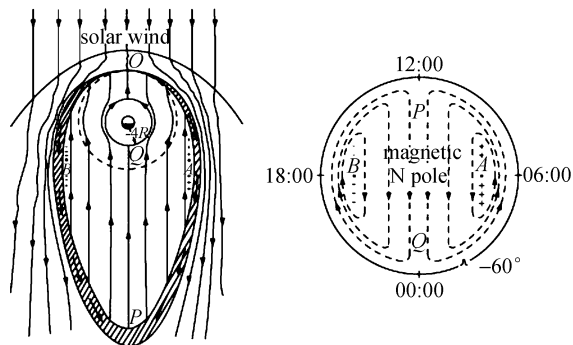


Figure 3 Viscous solar wind-magnetosphere interaction (Axford and Hines, 1961; Axford, 1963). Left panel shows a closed-magnetosphere with an upstream bow shock. The solar wind transfers antisunward momentum to the magnetosphere in a viscously interacting boundary layer. Right panel shows the motion of the footprints of the magnetospheric field in the northern ionosphere.

tool to revealing the magnetic field topology and flow characteristics, the uncertainty in field line tracing is large near the reconnection sites and, similarly, streamline tracing has large uncertainties in regions where flow undergoes significant changes, either associated with flow convergence/divergence or with a large velocity shear, and where the flow velocity is extremely small. Streamlines can form in regions even without physical flow using a streamline tracing software because the small numerical noise can provide non zero velocity for a streamline trace. The same tracing algorithm can sometimes be used to trace the current. Because the current is a derived quantity in a simulation, it may have larger errors than in the primary quantities especially in areas of weaker currents. For example, the currents are calculated from small perturbations of the strong background magnetic field resulting in a large uncertainty. These additional errors may mislead an investigation completely. In Subsection 3.3, we will discuss an example in which the simulation is flawed and an example in which the interpretation of the simulation is flawed.

2 Principles of Global Modeling

2.1 The Assumption

To link the large distances between regions of interest, global modeling assumes that the ideal Magnetohydrodynamics (MHD) is applicable in most places except in the reconnection sites and in the ionosphere, as well as in other regions of high collisions. In global modeling, we are interested in slow processes occurring in large spatial scales. In regions where the electromagnetic force is dominant, the communication between them is via the Alfvénic perturbations at the Alfvén speed V_A . The processes that occur more slowly than the Alfvén transit time, S/V_A , can be treated as quasi-steady state, where S is the spatial scale between the two regions. From steady state momentum equations of electrons, ions, and neutrals, one can derive a three-fluid Ohm’s law in the plasma frame of reference (Song *et al.*, 2001). Because in most magnetospheric and upper ionospheric regions the electron collision frequencies are much smaller than the electron gyro frequency, the electric conductivities are very large. In order to assure a finite

current in Ohm's law, the electric field resulting from plasma motion is

$$\mathbf{E}_{\perp} = -\mathbf{V} \times \mathbf{B}, \quad E_{\parallel} = 0, \quad (1)$$

where \mathbf{E} and \mathbf{V} are the electric field and the plasma bulk velocity measured in the same frame of reference and subscripts \perp and \parallel denote the components perpendicular and parallel to the magnetic field, respectively. Note that Equation (1) may not be valid when the electron bulk velocity is a few orders of magnitude greater than that of ions, a condition that may occur in regions of large field-aligned potential drop. Equation (1) is referred to as the ideal MHD approximation. Substituting the ideal MHD into Faraday's law, one can show that a fluid element carries the magnetic field with it as it moves and evolves in time. If the fluid element initially is with a bundle of magnetic field lines, or a so-called magnetic flux tube, the points along this flux tube will remain their relative positions as the flux tube evolves with time. This is the so-called frozen-in. Although the motion and distortion of the flux tube is caused by the plasma flow of each point along the field, it is convenient to think that the field line moves while being distorted, a concept that is useful but debatable (Vasyliūnas, 1972).

There is a common confusion between the ideal MHD approximation and the electric drift

$$\mathbf{V}_D = \mathbf{E} \times \mathbf{B} / B^2. \quad (2)$$

Equation (2) can be derived from Equation (1) when \mathbf{V} is perpendicular to \mathbf{B} and let $\mathbf{V} = \mathbf{V}_D$. In general, there is a field-aligned component of the velocity that cannot be determined by Equation (2). However, the ideal MHD approximation is only Equation (1) and not Equation (2). Note that the plasma bulk velocity used in global modeling is defined as the first moment of the distribution function which in principle includes multiple components of the plasma and should be derived from the plasma momentum equation. The velocity derived from Equation (2) may describe the flow velocity only if the plasma is dominant by a cold population. In general, one should not try to derive the flow velocity from the electric field. There is a significant difference in the causal relationship (Vasyliūnas, 2001) between Equation (1) and Equation (2). The electric field is self-consistently

produced (internally) by the motion of the plasma and cannot produce the plasma motion. Imposing an electric field externally will cause charge separation in the plasma. Net electric charges will occur at the boundaries where the electric field is imposed to form plasma sheathes in which the quasi-neutrality condition breaks down (Tu *et al.*, 2007). The external electric field will be shielded from penetrating into the plasma.

For example, when confused Equation (1) with Equation (2) and taking Equation (2) as the ideal MHD approximation, one would argue that because the drift velocity of the energetic particles in the ring current is associated with the gradient drifts and not the electric drift, Equation (2), the ideal MHD breaks down in the ring current region. However, we know that the ideal MHD approximation Equation (1) is valid for the ring current region because the electron collision frequency is negligibly small. The invalidity of Equation (2) is not the invalidity of the ideal MHD approximation. For energetic particles, the magnetic gradient force, $\nabla(\boldsymbol{\mu} \cdot \mathbf{B})$, should be included in the momentum equation, where $\boldsymbol{\mu}$ is the magnetic moment of a particle and in most global modeling problems is conserved. Their effect on the bulk velocity of the plasma depends on the concentration and energies of the energetic particles.

In general, the electric field is continuous across a quasi-steady state collisionless shock in the shock frame of reference although the processes taking place within the shock layer are not ideal MHD. In other words, the potential mapping method, which will be discussed below in detail, may be valid across a steady state shock.

How to treat the regions at reconnection sites and in the ionosphere in global modeling will be briefly discussed in Subsection 2.5 and 2.6.

Other localized regions where non ideal MHD effects are significant and cannot be neglected can be treated separately. The additional effects/processes can be added to the baseline ideal MHD description. In other words, the ideal MHD approximation is the foundation for global modeling and is not the only condition for global modeling to consider. In fact, to systematically include non ideal MHD processes in global modeling is an important task in any global modeling studies. One should not conclude

that global modeling does not work because ideal MHD approximation is invalid, a claim often made when one could not understand a simulation result.

2.2 Regions of Ideal MHD

In ideal MHD, because of the frozen-in condition, at a given moment, points on a field line move at their own flow speeds to form the field line for the next moment or next location in such a manner as illustrated in Figure 2(a).

In the regions where the ideal MHD approximation, Equation (1), holds, the electric field parallel to the magnetic field is zero. In other words, a field line, such as one in Figure 2(a), is equipotential. Similarly, the electric field parallel to the flow is also zero, or a streamline, such as one in Figure 2(c), is equipotential. If the field lines in Figure 2(a) are a time sequence of the same field line, or they are on the same set of streamlines, they all have the same electric potential. As a fluid element moves in space, the field lines that intersect the streamline of the element form a surface of equipotential. Fluid elements on different field lines or field lines from different streamlines have different electric potentials.

In quasi steady state, the electric potential difference between two field lines that are not on the same streamline remains constant as they travel through space while their shapes vary with time. This is the so-called potential mapping, the central element of global modeling when connecting distant regions. The electric potential difference between the two field lines equals $\int_{\mathbf{L}} (\mathbf{V} \times \mathbf{B}) \cdot d\mathbf{L}$ where \mathbf{L} is the distance between the two field lines of interest, such as that between two streamlines in Figure 2(c), at any given location or time. Since potential difference remains constant along two field lines as they map from one region to another, the electric field changes according to the distance between the two field lines. The motion of the plasma in one region can then be mapped to the other. If the two field lines are on the same streamline, \mathbf{V} and $d\mathbf{L}$ are parallel, resulting in zero potential difference.

One will have to use 3-D imagination to map the potentials described in Figure 2(a) and 2(c) in the solar wind and magnetosphere to that in Figure 2(b) in the ionosphere first from a straight line in the solar wind and then along 3-D (distorted) magnetic

dipole field lines to the ionosphere. If the streamlines shown in Figure 2(b) represent the footprints of the field lines above the ionosphere where the ideal MHD approximation remains valid, each streamline or convection line is an equipotential line and different streamlines have different potentials. The center of convection contours, or a convection cell, represents a peak or trough of the electric potential. The potential difference between the two cells corresponds to the cross-polar cap potential.

A basic rule of global modeling is that the field lines cannot intersect each other except at reconnection sites, or it will result in an infinite electric field at the intersection. Similarly, streamlines cannot intersect each other except at the reconnection sites, or resulting in an infinite electric field. Figure 2(a) and 2(c) show a good example of these concepts. Note that the streamlines converge (diverge) at the dayside magnetopause (nightside) reconnection line in Figure 2(c), but they do not intersect in other places. Similarly, the magnetic field lines in Figure 2(a) intersect in the reconnection regions.

The most important task for a specific model is to follow a given field line moving through the domain of interest, or to complete a full cycle of field motion within the domain. If this cannot be done for the model, there are inconsistencies in the model and the model is not valid for a steady state.

For the whole system, the magnetic influx, in terms of the number of magnetic field lines, equals the magnetic outflux. In the example shown in Figure 2(a), the solar wind field line that comes in from the dayside leaves the system after it is disconnected from the magnetosphere by reconnection on the nightside. If one foot of the field line, for example, remains connected with the Earth as the other foot convects with the solar wind to infinity, the system cannot reach a steady state. In other words, if a solar wind field line becomes connected with the Earth's field, it will have to be disconnected sooner or later in order to go back to the solar wind. A steady state global model with open field lines the feet of which forever convect in the polar cap is not self-consistent. This can be used as a criterion to quickly spot the problem of a model or simulation results.

In a dynamic process, the potential mapping needs correction. The correction is associated with

the induction term in Faraday's law and is determined by the change of the magnetic field and the time scale of the transition. Nevertheless, the total number of field lines that connect to outside field lines has to be the same before and after a dynamic process.

The concept of the streamlines is valid only in steady state; namely, when taking a snapshot, the velocity vector is tangent to the streamline everywhere and a fluid element on a streamline will move along this streamline afterward. In a dynamic process, when the flow undergoes significant changes, the lines formed by connecting velocity vectors at a given time is referred to as stack lines, which are what streamline tracing program provides in simulation diagnostics. A fluid element on a stack line may or may not follow the stack line at a later time. Therefore, extra caution needs to be taken when analyzing a simulation using simulation diagnostic tools in dynamic stages. Nevertheless, except in a few critical locations when the system undergoes rapid changes, by allowing some levels of uncertainty, streamline tracing can be a useful tool to diagnose the processes.

2.3 Motion and Distortion of a Magnetic Field Line

The motion of the plasma can be decomposed to a motion perpendicular to the magnetic field and a flow along the field. The perpendicular motion results in the motion of the field line and is driven (locally) by forces including the pressure gradient force, the curvature force (magnetic tension force) and the ionospheric coupling. The ionospheric coupling will be discussed separately in Subsection 2.6. The plasma motion mapping discussed in the last subsection corresponds to a magnetic tension force that results from the distortion of the flux tube because of the differences in the perpendicular velocity along it. Since the mapping assumes a steady state, it provides only a constant motion (Vasyliūnas, 2007). Its nature of a force will appear when there exist other forces and/or flow changes with which the tension force balances. Note that the electric field is not among the forces for an electrically quasi-neutral fluid. The electric drift, $\mathbf{E} \times \mathbf{B}/B^2$, cannot drive the flow and the electric field is a result of the field line motion as discussed above. That the plasma or the field lines can be driven by the electric field is one of the most common miscon-

ceptions in global modeling, although it often results in correct conclusions or models in steady states. The physical understanding and description is often incorrect.

Along the magnetic field, the flow can be driven by the pressure gradient force and the magnetic mirror force, as well as the gravity in mid- and high latitudes near the Earth.

A field line can be stretched or shortened if there is a velocity shear on different parts of a field line, or if the field-aligned velocity is not constant along a flux tube. After subtracting the average field-aligned velocity, if the flow diverges (converges), the field line is stretched (shortened). The parallel velocity difference between two elements on a field line, and hence the length of the segment of the field line, is equal, from mass conservation and magnetic flux conservation, to B/ρ , where ρ is the plasma mass density. We now look, for example, at the magnetosheath flow toward the magnetopause as indicated in Figure 4. If ignoring the effects of the magnetic field, the flow, in addition to being slowed down, diverges from the stagnation streamline and then is accelerated tangentially along the magnetopause boundary in the regions away from the subsolar. The Interplanetary Magnetic Field (IMF) frozen-in with the solar wind will experience distortion and stretching because of the velocity shear. The field line that touches the subsolar point is most interesting. Because the flow is stagnant at the subsolar point but the other two ends are connected to and convect with the solar wind, this field line in theory can be stretched infinitely unless there are some other processes, such as reconnection, to change the situation. The field lines on each side of the stagnant field line in Figure 4(a) will be slowed down and become curved around the subsolar point and drape, similarly but in lesser degrees to the stagnant field line, around the magnetosphere. When the effects of the magnetic field are included, the stagnation point of the magnetosheath flow shown in Figure 4, in steady state, extends along the stagnant field line to become a stagnation line (Sonnerup, 1974).

After passing around the dayside, in ideal MHD, the field lines will shorten themselves and accelerate, due to the curvature force. They will eventually catch up with the solar wind field lines they were originally

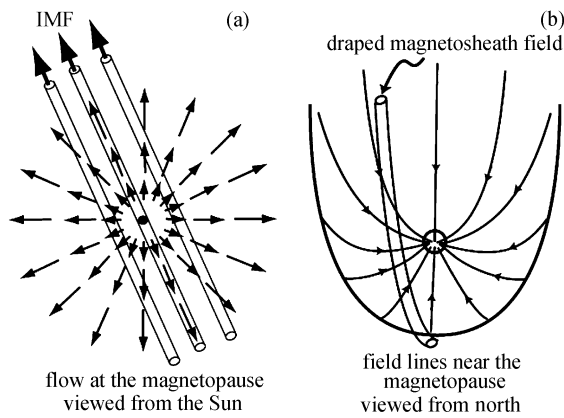


Figure 4 (a) Flow (small arrowheads) and IMF (tubes with big arrowhead) near the dayside magnetopause viewed from the Sun by ignoring the effect of the bow shock. To the lowest order, the magnetosheath flow diverges radially from the subsolar region. For a given IMF direction, the flow in the flux tube that drapes over the stagnation region is along the flux tube. The flux tube will not move from the stagnation region by such a flow. Flow in other flux tubes tends to carry the flux tubes away from the nose. (b) The field geometry near the magnetopause viewed from north. The magnetosheath flux tube drapes over the magnetopause and magnetospheric field bends due to push on the dayside and stretches on the nightside by the solar wind. A large field shear between the two occurs on the nightside of the cusp.

with before encountering the magnetosphere. Note that in this latter transient process, the field line can move faster than the solar wind speed.

The distortion of the field line can also be viewed in terms of wave mode, which helps to identify the types of the perturbations in observations and the dominating forces. The discussion given below is very useful in analyzing dynamic processes as well as the steady state processes which can be viewed as the long-time evolution of the dynamics.

There are 4 wave modes in the idea MHD: the entropy, slow, intermediate (sometimes referred to as the Alfvén mode), and fast modes, see Figure 5. The entropy mode is an often overlooked mode because when deriving the MHD dispersion relations, one often drops a factor of ω where ω is the angular frequency of the wave. This is a mode with $\omega = 0$, namely with phase velocity $\omega/k = 0$ where k is the

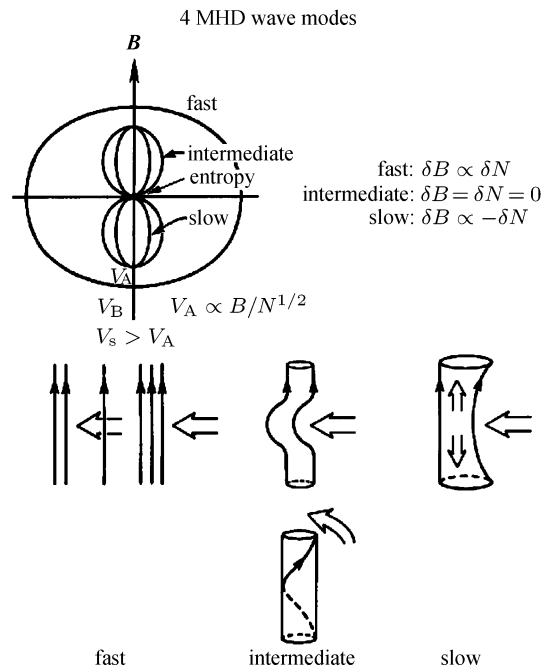


Figure 5 The four MHD modes, fast, intermediate, slow and entropy modes. Upper left panel shows the propagation speed for each mode as a function of the propagation angle relative to the magnetic field which points up, when the sound speed, V_s is greater than the Alfvén speed V_A . Upper right panel shows the characteristic perturbation relation for each propagating mode. Middle and lower panels illustrate the function of each propagating mode.

wave vector. This mode is none propagating, corresponding to force-balanced perturbations that are carried by the flow. Mirror mode structures are an example of the entropy mode.

Different modes not only have different propagation speeds, but also different perturbation relations, which can be used to identify the wave mode (Song *et al.*, 1994). In homogeneous plasma, the fast (slow) mode perturbations of the field strength are in (180° out of) phase with that in the plasma density. In the simplest case, the intermediate mode is incompressible (in both field strength and density).

To understand the physical functions of the three propagating modes, let us first examine the cause for each mode by assuming that the dominant forces in a system are only thermal pressure gradient force and the $\mathbf{J} \times \mathbf{B}$ force. In ideal MHD, the $\mathbf{J} \times \mathbf{B}$ force can be decomposed to a magnetic pressure gradient force and a curvature force. The intermediate mode,

because it is incompressible, results from the curvature force. There are two situations for the two pressure gradient forces. They can operate in phase to strengthen the net effects or they can operate 180° out of phase against each other. The fast mode results from the former situation. Because the net force is enhanced, the propagation velocity is higher, often resulting from/in a higher frequency. The slow mode results from the latter situation when the thermal pressure and magnetic pressure tend to cancel either other, corresponding to a slower propagation and often a lower frequency. Note that the frequencies referred to here are the frequencies in the plasma frame of reference.

We now examine the physical functions for each mode by applying a perturbation perpendicular to the magnetic field, as shown in the middle panel of Figure 5. For the fast mode, because it is the only MHD mode that can propagate perpendicular to the magnetic field, the perturbation will propagate perpendicular to the field as a pressure pulse with the magnetosonic speed. The field and the plasma are compressed or expanded in phase. For the intermediate mode, the field line will be bent and the perturbation will propagate more parallel or antiparallel to the field. If the initial perturbation is sustained, the whole field line will be straightened and shift to the left to reach a steady state. If the perturbation is a pulse, the whole field line will oscillate. The function of the slow mode is most interesting. The initial perturbation will compress the magnetic flux tube at the center. The field strength will increase as the cross-section decreases. However, the plasma density has to decrease as required by the slow mode perturbation relation. The only way to achieve this is to create field-aligned flows from the region of the initial perturbation. In effect, the slow mode converts a perturbation from perpendicular to the magnetic field to parallel (and antiparallel) to it. The plasma is squeezed out of the flux tube. Noting that the flow diverges from the center, as discussed above, the field line is stretched. This can be confirmed by an increase in B/ρ .

Combining the perturbation relations with the field line length relation, we conclude that the slow

mode is most effective in stretching and shortening a field line and the intermediate mode in bending and twisting a field. The fast mode is most effective to accelerate/decelerate the flow perpendicular to the field in high β plasma, where β is the ratio of the thermal pressure to the magnetic pressure, because it is the only propagating mode perpendicular to the magnetic field. The intermediate mode, or Alfvén mode, is most efficient for low β plasma.

The pure Alfvén mode is least effective in stretching or shortening a field line, from the field line length definition and the Alfvén mode perturbation relation. When a highly stretched field line is shortening, say, the outflow region after reconnection, the modes involved most likely are the slow modes, although the intermediate/Alfvén mode is often attributed to the shortening. In fact, in the outflow region because the field strength will decrease as the magnetic energy is converted to plasma kinetic energy after reconnection and the density has to increase as required by the slow mode perturbation relation, B/ρ or the field line length decreases. The earthward flow after tail reconnection is a more complicated problem because it involves a nonuniform field the strength of which depends on the distance from the Earth.

2.4 Bending and Foot Motion of a Dipole Magnetic Field Line

The near-Earth magnetic field can be well approximated by a dipole field with some modifications. The dipole field is special because its field line is curved and, however, it is a curl-free field since there is no current in regions away from the dipole. The magnetic pressure gradient force is canceled by the curvature force everywhere. The characteristics of the wave modes discussed in the last Subsection 2.3 need significantly modified.

Let us consider a poleward motion at the foot of a dipole field line as indicated in Figure 6. With the bending of the field line, a pair of currents is produced on the two sides of the kink of the magnetic field. Above the kink in higher altitudes, the $\mathbf{J} \times \mathbf{B}$ force associated with the current acting on the dipole field tends to push the field line to the dipole field line at a larger L -shell as the kink propagates to higher altitudes. Note that when the field line reaches the

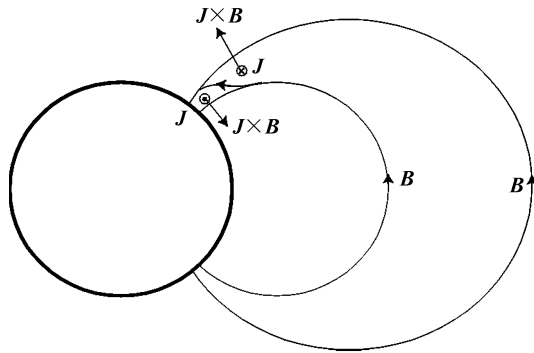


Figure 6 A dipole magnetic field with a poleward perturbation at a foot. The currents, \mathbf{J} , produced by the perturbation are in or out of the plane and the $\mathbf{J} \times \mathbf{B}$ force is poleward (equatorward) above (below) the kink in the field line.

dipole field line at this larger L -value, the current and hence the cause of the motion diminishes. (In a more detailed description, the perturbation will propagate to the conjugate ionosphere and may be reflected back and forth a few times before the energy contained in the perturbation is completely dissipated in the ionosphere). Below the kink, on the other hand, the $\mathbf{J} \times \mathbf{B}$ force tends to push back the field to its unperturbed geometry. If the original cause of the perturbation is not sustained, the perturbation will propagate as a pulse along the field line, similar to the intermediate mode perturbation in uniform field as discussed in the last section. If the original perturbation can be sustained, *i.e.*, there is a continuous poleward ionospheric flow, the field line will reach a steady state in this new L -shell. Here we have ignored the redistribution of the plasma in this process which may produce a pressure gradient force to react back on the motion.

Ideally, if the original perturbation is perpendicular to the magnetic field, the field line is not stretched but becomes longer purely because of the characteristics of the dipole field. This situation may correspond to the intermediate mode perturbation for a uniform magnetic field. As the flux tube expands in the absence of parallel flow, because the equatorial field strength decreases, the plasma density decreases proportionally to the magnetic volume $\int_s ds/B$, where ds is length the field line, from the magnetic flux and the mass conservations. Since the length of a dipole

field line is proportional to the L -value, the intermediate mode perturbation relation in the dipole field is modified as $B/L\rho_e = \text{const}$ where ρ_e is the equatorial density.

However, the above description is highly simplified. One may consider the feet of the flux tube are rooted in the E-layer ionosphere. The ionosphere density peaks at the F-layer. In the mid- to low latitudes, the motion perpendicular to the magnetic field to larger L -value has an upward component of motion. Therefore, as a result of the poleward motion of the field line, an additional portion of the field line is pulled out of the ionosphere (with high density plasma) although we have not invoked a field-aligned flow velocity. The ionosphere, especially in low latitudes, would appear to rise. As the ionosphere rises, the gravity force comes into play and results in the Appleton anomaly. Note that in this process, there is no electric field imposed in the azimuthal, *i.e.*, east-west, direction, which is the conventional explanation of the upward motion of the dayside equatorial ionosphere during magnetic storms although, again as we have discussed, the plasma flow cannot be driven by the electric field. In fact, the field lines are not vertical except at the poles. The poleward motion of the foot of a field line has a downward component. This effect will partially offset the density increase in the ionosphere.

Let us now consider the ionospheric horizontal motion, the central issue for global modeling. At the foot of a field line, the ionosphere can be approximated as a nearly incompressible flow for global modeling purposes (because the critical time scale for the fast mode traveling in the ionosphere, which is the spatial scale of the ionosphere divided by the fast mode speed, is much smaller than the magnetospheric MHD time scales). In the discussion below, we will include this small effect of compression. But loosely speaking, the ionosphere velocity can be treated as divergence-free, from mass conservation, and a streamline needs to be closed. This is different from the magnetospheric streamlines that can converge or diverge at reconnection sites, as discussed above.

On the dayside, the poleward motion of a closed

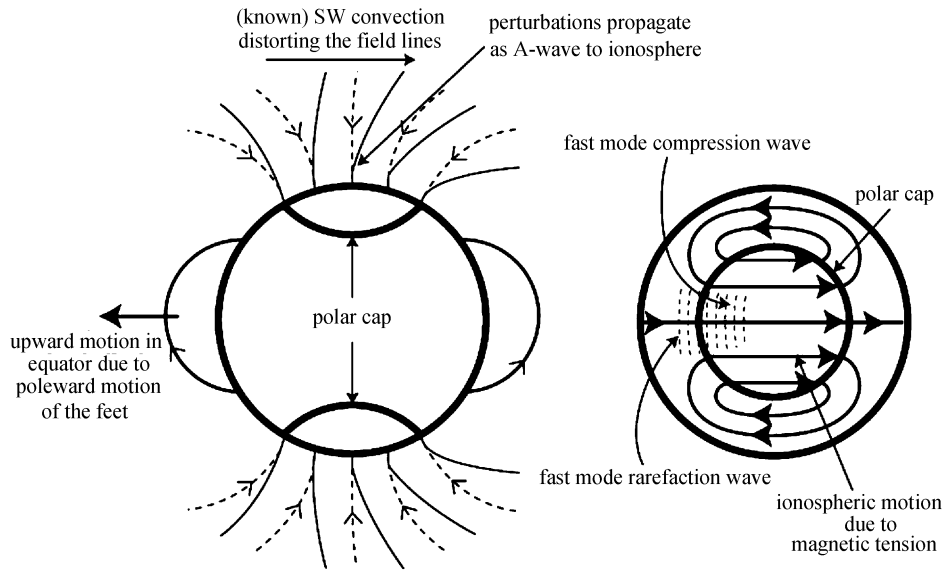


Figure 7 The magnetic field and plasma motion in and near the ionosphere. (a) Dashed lines with arrowheads indicate undisturbed Earth's magnetic field in the noon-midnight meridian plane. Solid lines in the two polar regions indicate the field lines perturbations when they, after reconnection, are driven by the solar wind. (b) Solid lines with arrowheads indicate the convection in the northern ionosphere.

field line can be caused by the antisunward motion of an open field line that is dragged by the solar wind flow, as shown in Figure 7. In the ionosphere, the enhanced antisunward flow at the footprint of the reconnected field line creates a compressional fast mode wave that quickly propagates through out the ionosphere. On the dayside closed-field region (lower latitude to the reconnected field lines), the perturbation in the ionosphere is fast mode rarefaction. The convection forms closed convection cells in order to satisfy the mass conservation requirement, as discussed above. The poleward motion of closed field lines produces upward motion in the equatorial region near local noon. This upward ionospheric motion has sometimes been interpreted as a result of a penetration electric field which cannot be derived according to the global modeling principles. According to the global modeling principles, the electric field can only be a result of the poleward motion of the flux tube given by Equation (1), as we have emphasized repeatedly due to the wide spread misconception.

Similarly but reversely, on the nightside, tail reconnection produces an equatorward motion at the feet of the first closed field line as it shortens itself and moving earthward, resulting in downward motion of the equatorial ionosphere if a significant ionospheric

F-layer exists. This downward motion corresponds to a westward electric field, which has been interpreted as the cause of the downward motion. Again, the nightside downward motion of the equatorial ionosphere is a result of the equatorward motion of the field lines according to the principles of global modeling.

If the dipole field is pushed, instead of at the ionosphere, far from the Earth in the equatorial region, such as when a high-pressure front pushes the subsolar magnetopause inward, in a similar analysis, the field line will move to a small L -shell and the field line is shortened. If the pressure pulse front is very sharp, in the time scale shorter than the Alfvén time, a bulge of the field line may potentially develop if the plasma pressure is relatively high before the arrival of the front. The plasma is squeezed from the equator and accumulated to form a high pressure region just upstream of the incoming front. However, this field line bulge cannot stay after the front pushes through the magnetosphere because the front will not stay and will convect to the nightside and because the pressure gradient will produce field-aligned flow as discussed above.

A similar analysis can be applied to the corotation of the magnetosphere by assuming that the push

is produced by the E-layer neutral wind moving in the azimuthal direction.

2.5 Reconnection Region

The ideal MHD approximation breaks down in the diffusion region of reconnection. This condition has been used by some to argue for inconsistencies in some models. For instance, some argued that because the ideal MHD breaks down, an electric field could exist along the magnetic field. Effects due to 3-dimensionality are another area sometimes used to argue in order to get around the difficulties faced by some models. As we will see, most of these arguments are inconsistent with the principles of global modeling.

It is true that there remain unknowns about the details of the reconnection process although it is the most powerful mechanism to change magnetic topology and to convert magnetic energy to kinetic energy and possibly to thermal energy in collisionless or weakly collisional plasma. Nevertheless, for the purposes of global modeling we assume that in only a limited spatial region ideal MHD is replaced with resistive Ohm's law. This limited region is most likely to be around a curvy thin line with a certain length. A 3-D situation may be simplified to a 2-D situation by choosing a curvilinear coordinate system with one axis along the thin reconnection line. For simplicity, we base our discussion on the Petschek's (1964) reconnection model, Figure 8, which is 2-dimensional and both the magnetic field and the plasma velocity have no component along the reconnection line. Although the reconnection rate may be model dependent, it is clear that the mass and magnetic flux into the reconnection site and out of it are conserved. It is important to point out that beyond the small diffusion region, ideal MHD is applicable in both inflow and outflow regions. Therefore, any violation of ideal MHD is negligible except in the diffusion region and one should not expect any magical processes to produce appreciable effects in MHD time scales, such as a large field-aligned potential drops along a flux tube in the outflow region.

The electric field in the 2-D model, Figure 8, points out of the page in all three regions: the diffusion region, inflow region and outflow region. The difference is that in the ideal MHD regions it equals

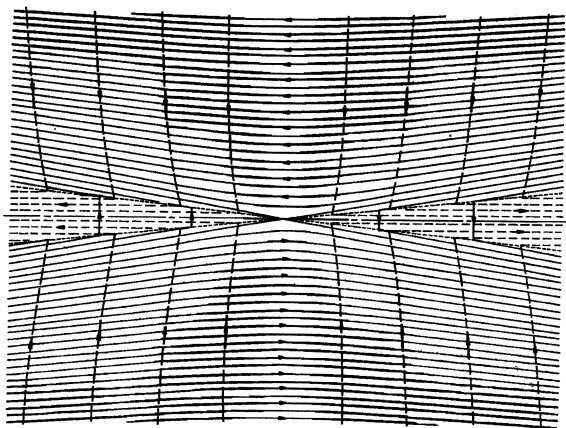


Figure 8 Petschek's two-dimensional reconnection geometry (Vasyliūnas, 1975). At the center is the diffusion region to which the influx converges from top and bottom, as indicated by dashed lines with arrowheads. The outflux diverges from the diffusion region to the right and left. The magnetic field is indicated by solid lines with arrowheads. The 4 dashed lines radiating from the diffusion region indicate the slow shocks, the center piece of the Petschek's model. They are sometimes confused with the separatrices in kinematic reconnection models. The magnetic field lines go through the shocks but not separatrices.

$\mathbf{V} \times \mathbf{B}$ and in the diffusion region it equals \mathbf{J}/σ where σ is the conductivity and \mathbf{J} is determined from the magnetic field change across the reconnection region. In steady state, the electric field is constant in space. Therefore, the potential difference between two field lines at different locations along the reconnection line, the y -direction, remains the same before they convect into the reconnection region and after they convect out. This condition is used in global modeling for electric potential or plasma motion mapping.

By careful examination of Figure 8, one finds that almost all field lines do not connect directly to the reconnection site except the ones on the separatrices. Even for these reconnecting field lines ideal MHD approximation is valid except for a small segment in the diffusion region.

Note that although the fluid and field lines shown in Figure 8 are steady state, it is a snapshot at a given time. The fluid elements or field lines are moving with time. At the next time, although the flow pattern and the field line geometry looks the same, the fluid

elements one has followed would have changed their locations. The field lines move into the reconnection region and convect away. They do not stay still as described in certain static or kinematic reconnection models. In the process when these field lines convect from inflow regions to outflow regions, only a very small segment of a field line goes through the diffusion region for a very short period of time when ideal MHD breaks down. Therefore, for the purposes of global modeling, reconnection only changes the topology of a field line and creates a large curvature force in the outflow region which accelerates the flow to the local Alfvén speed.

When reconnection is impulsive and cannot be treated as steady state, the resulting outflow speed may fluctuate, but the average speed is controlled by the solar wind speed and the antiparallel component of the IMF flux as well as the local plasma conditions, because over time the solar wind field lines that participate in reconnection are carried by the rest of the solar wind flux tubes, as the streamlines on these field lines in the solar wind cannot cross each other except in a solar wind current sheet where reconnection may take place within the solar wind.

If there is a uniform velocity along the reconnection line in the simple 2-D Petschek model, one can always make a frame transformation to remove the effect of the flow effect.

If there is a uniform component of the magnetic field along the reconnection line, such as that described in certain reconnection models, although there are other effects of this field on the reconnection process, the reconnection electric field described in the above 2-D model will have a component along the magnetic field and produce a field-aligned electric potential drop which can accelerate or decelerate the plasma along the magnetic field. From the global modeling point of view, the convection speed of the field lines, namely the perpendicular velocity, remains the same as that without the field component along the reconnection line. We should point out that, based on the observed ionospheric convection which is proportional to the coupled potential from the solar wind, the reconnection line is a few R_e long and that, based on in situ observations, the reconnection region has very small spatial scales in the two dimensions perpendicular to the reconnection line, implying

that reconnection process can be described well in 2-D models at least for the purposes of global modeling. We note that 3-D effects refer to processes when the reconnection line is of the same length scale as the two perpendicular dimensions and not refer to effects associated with the field or velocity that has a component along the reconnection line. Heavily relying on 3-D effects of reconnection in a global model may indicate an inconsistency in the model.

2.6 Magnetosphere-ionosphere Coupling

The ideal MHD approximation also breaks down in the ionosphere because of the high collision frequencies of the plasma with the neutral particles. Vasyliūnas (1970) and Wolf (1970) proposed a model to couple the magnetospheric motion to the ionosphere by using Ohm's law in the ionosphere, see Figure 9(a). In this treatment, the ionosphere is approximated as 1-dimensional but allowing current to flow into or out of it along the magnetic field lines. Assuming that over the whole ionosphere, the field-aligned currents continuously converge or diverge to become horizontal currents, they, as required by the current conservation, become and are linked by the (height-integrated) horizontal Pedersen currents. Height-integrated Ohm's law relates the Pedersen currents with the Hall currents and horizontal electric field. Therefore, the magnetospheric motion is mapped to the ionospheric motion and eventually is mapped as the ionospheric potential. Because in steady state, the electric potential in the ionospheric setting can be relatively easily solved from the Poisson equation, it has been widely used as a shortcut to derive the ionospheric motion. Although most of the measurements are made from the ionospheric convection, they are converted into and discussed in terms of electric fields. Even as we pointed out above that the electric field will be shielded by the plasma, terminologies, such as penetration electric field are widely used as drivers of ionospheric and even magnetospheric motions.

This coupling scheme has worked remarkably well as a foundation for many models and theories. For example, most of the global MHD simulation models use the scheme with some minor modifications. In global MHD simulations, because the Alfvén speed becomes very large just above the ionosphere, where the field is strong while the plasma density is

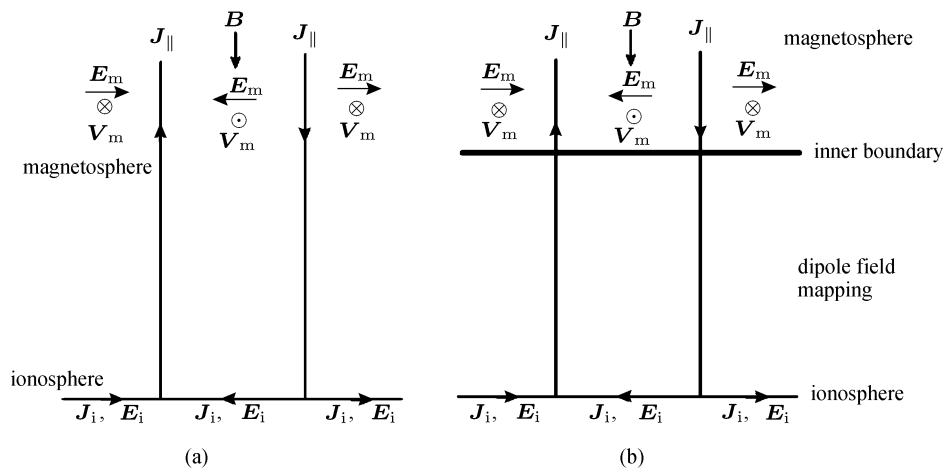


Figure 9 Magnetosphere-ionosphere coupling in the northern polar region. (a) The original models (Vasyliūnas, 1970; Wolf, 1970) couple the magnetosphere electromagnetic fields and currents to a height-integrated ionosphere. (b) In global simulation models, the magnetospheric MHD simulations end at an inner boundary a few Earth radii above the ionosphere. The electric fields and currents are mapped between the magnetosphere and a height-integrated ionosphere.

low, the simulation models have to set the inner boundary of the simulation domain at a few earth radii above the Earth, as shown in Figure 9(b). The field-aligned current and the electric field between the inner boundary and the ionosphere are mapped via a dipole magnetic field. Important approximations in this treatment are that Ohm’s law used is in the frame of reference of the neutral wind and that the ion motion is assumed steady state. Therefore, this approach is not valid for dynamic processes and the neutral wind velocity cannot be self-consistently derived both in height and in time. Applications of this treatment to dynamic processes such as substorms need to be especially cautious.

3 An Example of Applications: Global Modeling for Northward IMF

3.1 Review of Critical Issues

The global modeling for northward IMF is a very difficult problem. Two years after proposing the global model for southward IMF, Dungey (1963) proposed a model for northward IMF, see Figure 10. Note that the concept of the magnetopause was not firmly established at the time. Here we start with a northward IMF line that convects along the Sun-Earth line toward the Earth from the dayside and after interaction with the magnetosphere goes back to the solar

wind on the nightside. On the dayside, in the subsolar region, the solar wind flow slows down as it approaches the magnetosphere. Because the two ends of the IMF continue to move at the solar wind speed, the field line drapes over the magnetosphere. Dungey perceived that reconnection between the IMF and the magnetosphere might take place on the nightside in both hemispheres where the magnetospheric field and IMF are antiparallel. Reconnection at the two lobes forms a closed field line on the dayside and a detached field line. The kinks created on the newly formed closed field line produce sunward convection in the polar magnetosphere and ionosphere. The kinks on the newly detached field line accelerate the field line to catch up with the rest of the solar wind. In the nightside closed field line region, in order to supply the inflow to reconnection, the ionospheric motion is

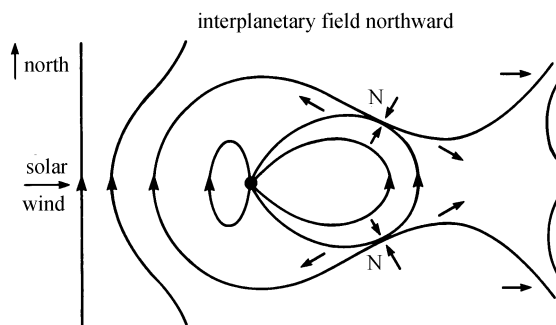


Figure 10 Global geometry for northward IMF (Dungey, 1963).

poleward, or sunward. Note that the field lines and flow are consistent with the principles discussed above, especially when following a field line going through the system, although the locations of reconnection are slightly different from nowadays perception. There are two issues that are not clear in this figure. The first issue is the convection of the outer magnetosphere. Following the newly closed field line, one can derive from the figure that it becomes the dayside closed field line, an antisunward magnetospheric motion and an equatorward ionospheric convection. This field line may go around the Earth and become the near-earth closed field line that eventually expands to become the reconnection field line. We will see later that the key equation is how close to the Earth this antisunward flow can become. The second issue is about the field line motion that is not in the noon-midnight meridian plane and the flow pattern in the equatorial plane and that in the ionosphere; they need to be consistently mapped according to the principles discussed above. Because the field lines described in the model are on the same streamline, they are equipotential.

These two issues are obviously too difficult to address from a pure theoretical point of view. The clues to the answers of these issues can be provided by observations. Antisunward flow has never been observed in the outer magnetosphere even today. In other words, there was a good reason for Dungey to be unspecific on the first issue. The first important observation was the observation of the Low-Latitude Boundary Layer (LLBL) (Eastman, 1979), in which the magnetosheath plasma was found in the magnetosphere moving in the antisunward direction with a fraction of the solar wind speed. Note that this antisunward flow is not observed in the Sun-Earth line but along the flank of the magnetopause. Because the temporal resolution of the original measurements was very low at the time, the layer was interpreted as diffusive and viscous in nature. Historically, this interpretation had led to extensive investigations of enhanced viscosity and diffusion coefficients via various waves or turbulences. However, the investigations had drawn a negative conclusion that the amplitudes and spectra observed near the magnetopause cannot provide enough, by a large margin, anomalous

viscosity or diffusion required by the observed LLBL properties (*e.g.*, Sonnerup, 1980a, b; Treumann *et al.*, 1995), an interesting example of the interpretation of an observation misleading theoretical and modeling efforts. Note that to estimate the linkage between the two, one needs follow the global modeling principles, an excellent example of global modeling leading the theoretical investigations. With the improvement of the particle detectors, the LLBL for northward IMF is more often observed as layers with relatively gentle density gradients but sharp changes at the boundaries (Song *et al.*, 1990, 1993). These observations have led to investigations of other solar wind entry mechanisms, such as reconnection.

Song and Russell (1992) proposed a model of the formation of the LLBL for northward IMF. They first analyzed the flow diversion and field distortion near the subsolar region as discussed in Figure 4. They recognized the fact that the flux tube along the stagnation streamline cannot leave the system unless some other processes take place as discussed above. This other process could be reconnection. If reconnection takes place in both hemispheres, similar to the Dungey's original proposal (1963), the magnetosphere effectively captures an IMF flux tube with its solar wind content, see Figure 11.

The newly formed flux tube has its main portion outside of the magnetopause with the two feet connect to the Earth. There must be kinks on the field line where it threads through the magnetopause. The kink, one on each hemisphere, will propagate toward the equator as shown in Figure 12, when the flux tube "sinks" into the magnetosphere. Note that although this wave front is referred to as the Alfvén mode, it should be compressional if the magnetospheric field is stronger than the magnetosheath one when the flux tube is compressed as moving into the magnetosphere.

The newly captured solar wind flux tube still does not make the LLBL. Song and Russell (1990) analyzed the situation of the flux tube and found that it is unstable to interchange instability. It is obvious that as the flux sinks into the magnetosphere, it is shortened in length and compressed in diameter. The plasma density, and hence the pressure, is higher. This flux tube with a higher pressure has a tendency

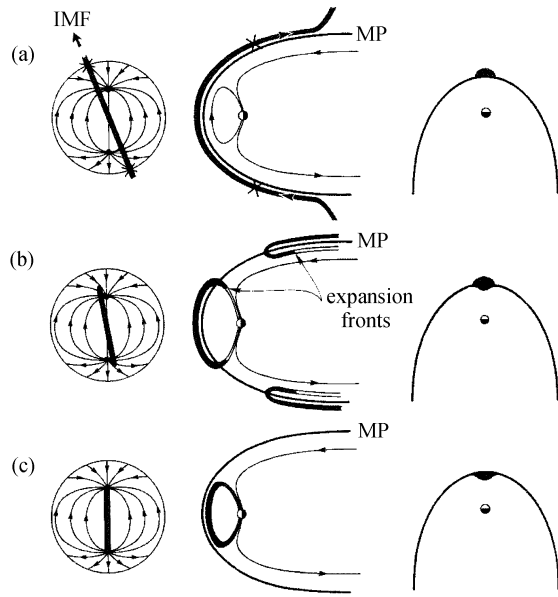


Figure 11 The LLBL model proposed by Song and Russell (1992). The three plots in each panel are the magnetosphere viewed from the Sun, the magnetosphere cut in the plane containing the IMF and Sun-Earth line, and the equatorial plane of the magnetosphere. (a) A massive magnetosheath flux tube, shaded areas, reconnects with empty lobe flux tubes on the nightside of the cusps indicated by big crosses. (b) The dayside branch of the reconnected flux tube shortens while magnetosheath particles start propagating into the empty magnetospheric portion. The disconnected portion also shortens and convects away with the solar wind. (c) The flux tube stretches (more toward the noon meridian) and sinks into the magnetosphere.

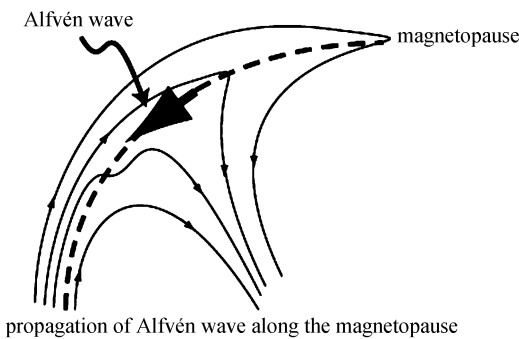


Figure 12 Sinking of the newly captured magnetosheath field seen in a noon-midnight cut. The field lines are indicated by thin lines with arrowheads. The magnetopause current is shown by the dashed line. The kink of the field line propagates along the magnetopause from high latitudes to low latitudes as indicated by a big arrowhead. This corresponds to an Alfvén wave front.

to expand. It cannot expand outward because this is where it came from. If it expands toward the Earth, the field line will be shorter and the diameter will be smaller because of the stronger field closer to the Earth. This is not an expansion but a compression and will not naturally proceed. An interesting fact is that the shape of the magnetopause decreases in the curvature from the noon to terminators. Therefore, the flux tube can expand sideways along the magnetopause. This motion corresponds to the interchange instability which converts potential and thermal energies into kinetic energy. The flow is accelerated, see Figure 13. If reconnection is time dependent, multiple layers of the observed LLBL can be formed. If reconnection is steady state, the effective process is that the (shocked) solar wind continuously flows into the magnetosphere and moves along the magnetopause. There have been overwhelming observational evidence to support the model, in contrast to alternative mechanisms, since it was proposed. Nevertheless, this model, although explained the formation of the LLBL, still is a local model and does not address globally the magnetospheric and ionospheric processes. The important progress is that we started understanding the process in the magnetosphere away from the noon-midnight meridian plane. It removes the possibility of an antisunward flow through the magnetosphere as we discussed above concerning Figure 10.

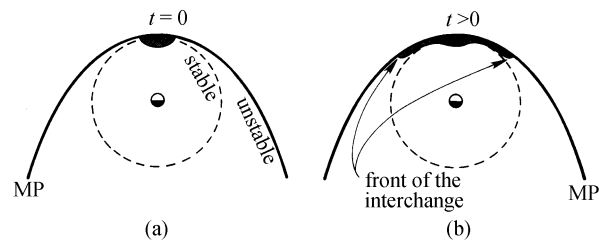


Figure 13 Consequence at the equatorial plane after the newly captured flux tube sinks into the magnetosphere (Song and Russell, 1992). (a) A flux tube containing magnetosheath particles with higher pressure. (b) The flux tube disperses and expands azimuthally via the interchange instability and forms a boundary layer. The shaded curves indicate where the field has the same magnetic volume as the subsolar point on the magnetospheric side of the magnetopause current layer. Interchanges earthward to the dashed curve are stable to the interchange instability and will not proceed.

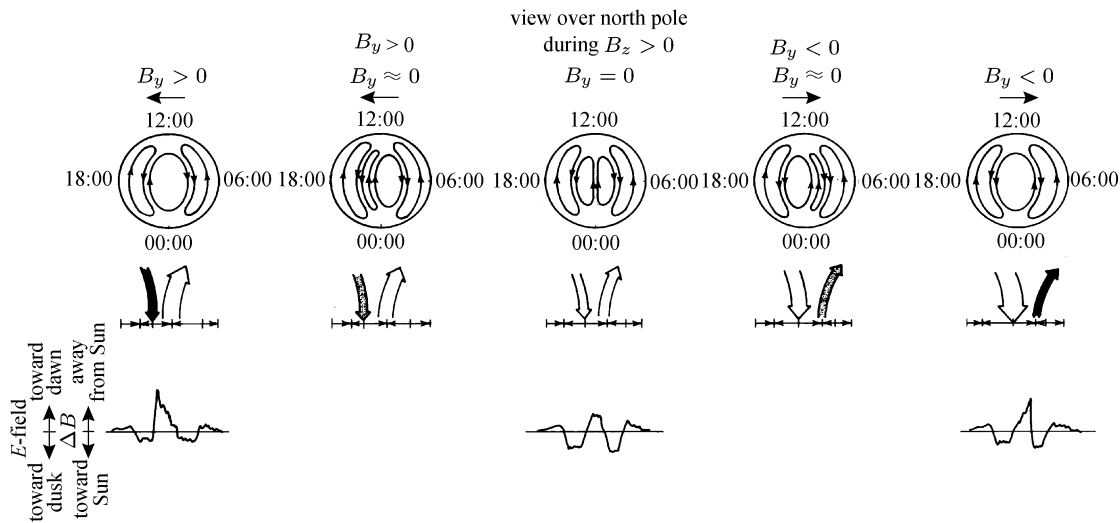


Figure 14 Summary of ionospheric observations of convection (upper panel), field-aligned currents (middle panel), and the magnetic field perturbations (lower panel) for northward IMF with various B_y components (Potemra *et al.*, 1984).

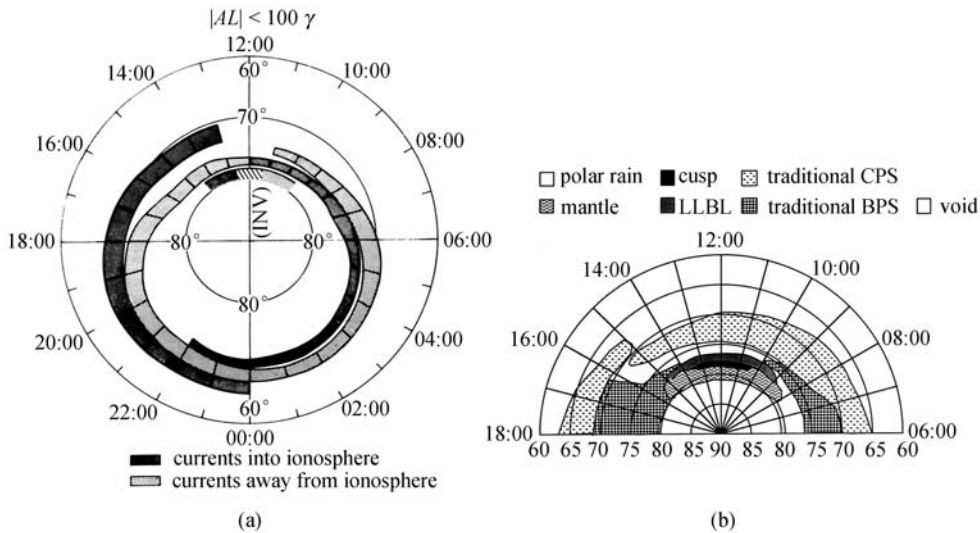


Figure 15 (a) Polar field-aligned currents for northward IMF (Iijima and Potemra, 1976), and (b) polar precipitation particle observation for northward IFM (Newell and Meng, 1994).

To understand the global processes, ionospheric observations are crucial. Over the years, a clear picture of the polar ionosphere gradually emerged from observations for northward IMF, see Figure 14. There is an additional pair of convection cells poleward of the antisunward convection cells with a polarity opposite to them. They are referred to as the reverse cells. There also appears a pair of field-aligned currents, known as the NBZ currents, with an opposite polarity to and on the poleward side of the region 1 currents, see Figure 15(a) (Iijima and Potemra, 1976). Furthermore, the cusps, where most precip-

itation is observed with solar wind origin, appear to be located between the NBZ currents and region 1 currents around local noon, see Figure 15(b) (Newell and Meng, 1994).

With these new observations, various models were proposed to explain some of them (*e.g.*, Reiff and Burch, 1985; Kan and Burke, 1985; Siscoe *et al.*, 1991; Burch *et al.*, 1992; Crooker, 1992). At the same time, computer simulations had left its infancy and grew up to become a toddler. They started providing sometimes useful while other times confusing information. For northward IMF, most of the global sim-

ulation models showed that reconnection takes place in the cusps with a closed magnetotail (Ogino and Walker, 1984; Usadi *et al.*, 1993; Ogino *et al.*, 1994; Fedder and Lyon, 1995; Gombosi *et al.*, 1998; Bar-gatze *et al.*, 1999; Song *et al.*, 1999; Raeder, 1999; Watanabe *et al.*, 2005), except one which showed an additional reconnection site in the tail with an open magnetosphere (Raeder *et al.*, 1995). We will discuss the latter possibility in Subsection 3.3.

With these clues from observations and simulations, most important questions for a modeler are: Is the magnetosphere open or closed? What is the driver of the sunward ionospheric flow, as well as the antisunward flow? From the discussion above, it is obvious that the Dungey's (1963) model can provide sunward convection and that his model gives a closed magnetosphere, while Song and Russell model (1992) left the status of the nightside magnetosphere undetermined. One key issue related to the antisunward convection cells is the term it has been referred to: the viscous cells (Kan and Burke, 1985; Burch *et al.*, 1992). This was because their flow direction seems to be related to the solar wind. If this were true, the ionospheric region poleward of the viscous cells would map to the open field region and connect to the solar wind. In this case, the ionospheric convection could not be sunward. If a model assumed an antisunward flow driven by the solar wind in lower latitudes and a sunward flow at higher latitudes near the noon-midnight meridian, somewhere between the two, the global modeling principles would have to break. In other words, one could not follow a field line going through a whole cycle of convection in such a model. Somewhere other than standard reconnection regions the field lines and streamlines would have to cross each other, an unavoidable inconsistency and the breakdown of the model.

3.2 A Global Model for Northward IMF

Figure 16 shows, as an example of how to apply the principles of global modeling, a possible steady state of the magnetosphere for northward IMF with its ionospheric mapping according to the global modeling principles. The magnetosphere consists of three major regions: The plasmasphere (pink region), the outer magnetosphere (yellow region), and the LLBL/tail (blue region). The latter two regions are

shown with ionospheric mapping. The plasmasphere is mapped to lower latitudes of panel *c*. One has to use 3-D imagination along a (distorted) dipole field to construct the relationship between the three panels. The plasmasphere is a doughnut-shaped region. The outer magnetosphere has a similar shape to the plasmasphere but envelopes it while squeezed slightly on the dayside and stretched a little on the nightside. The LLBL/tail region envelopes the outer magnetosphere and is bounded by a teardrop-shaped outer surface of the magnetopause. In ideal MHD steady state, the three regions are topologically separated by boundaries, or mathematical separatrix surfaces. In other words, streamlines do not penetrate from one region into the others. The LLBL/tail region connects with the outside (the magnetosheath) by reconnection at the two cusps and is directly driven by the entered solar wind as discussed in Subsection 3.1. It maps to the two polar cap regions, but it is on closed field lines except in the cusps. (The notion that the polar cap is on open field lines is an over simplified and, in this case, incorrect statement) The magnetospheric flow in this region is antisunward, similar to what proposed by Dungey (1963) but it does not go into the dayside magnetosphere. Its ionospheric flow, on the other hand, first diverges from local noon as expected from the mapping of the LLBL, then converges to the midnight, corresponding to point *b*, and eventually returns to higher latitudes as the magnetotail flow moving away from the Earth. This forms a pair of convection cells in the polar ionosphere, corresponding to the reverse cells and NBZ currents. The antisunward convection is driven by the high pressure near local noon as described by Song and Russell (1992) model. The sunward convection in the ionosphere corresponds to the antisunward equatorial flow from point *b* to point *a* in Figure 16 when the two corresponding field lines map to the ionosphere, and is driven by the combination of the tailward convection associated with the LLBL and the rarefaction wave associated with reconnection poleward of the cusp, point *a* in Figure 16(c).

The outer magnetosphere is topologically isolated from the field and particles of solar wind origin unless diffusion at the magnetosphere-LLBL/tail boundary is important. It consists of a pair of cells

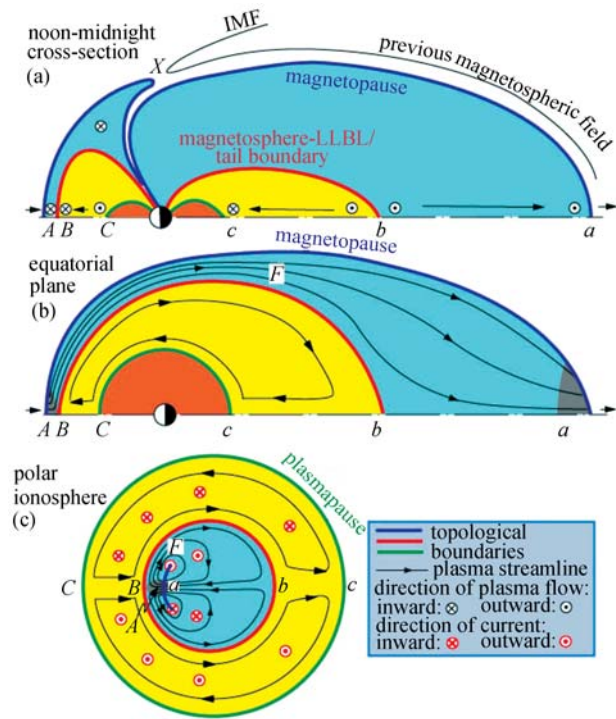


Figure 16 Global geometry of the magnetosphere and ionospheric mapping (Song *et al.*, 1999). In all panels, thick solid lines represent the separatrix surfaces and thin solid lines with arrowheads indicate the direction of the flow, and the heavily shaded areas indicate the regions ambient to newly reconnected/disconnected magnetic field lines of which the topological status is ambiguous. (a) The noon-midnight meridian plane of the magnetosphere viewed from dusk. Circles with crosses (dots) indicate the plasma flows away from (toward) the reader on the morning side, but is diverted before reaching the noon-midnight meridian plane. The magnetopause/cusp is the surface consisting of curves $A-X$ -Earth on the day-side and Earth- a on the nightside. The boundary between the outer magnetosphere and LLBL/tail consists of curves B -Earth on the dayside and Earth- b on the nightside, and the plasmopause consists of curves C -Earth and Earth- c . (b) The equatorial plane of the magnetosphere viewed from north. Point F indicates where the boundary layer streamline turns from away from sun-Earth line to toward the sun-Earth line, and maps to the ends of the cusp arc in panel c . (c) The northern ionosphere viewed from top. The circles with dots and crosses indicate the directions of the field-aligned currents, instead of the plasma flows.

in the magnetosphere that map to the ionosphere as the “viscous” cells and region 1 currents. However,

they are not driven by the viscosity. According to the global modeling principles, there is no interaction possible in ideal MHD between the outer magnetosphere and LLBL/tail regions. What can drive the convection? Although LLBL region has an antisunward flow, how can the outer magnetosphere move in the same direction if ideal MHD does not break down? The ideal MHD does break down but not in the magnetosphere. Instead, the breakdown occurs in the ionosphere. As shown in Figure 17, the NBZ field-aligned currents (the middle pair of J_{\parallel}), of which the driver has been identified above, diverge/converge at the ionosphere to become the Pedersen currents. The currents can go across the separatrix (the thick vertical lines) under the topological boundaries in the ionosphere. Part of the energy carried by the currents is dissipated and the remaining couples to the region 1 currents (the J_{\parallel} on two sides). The Ampère force of the Pedersen currents, $J \times B$, drives the ionospheric convection in the same polarity as the viscous cells, as shown in Figure 17. Note that in the steady

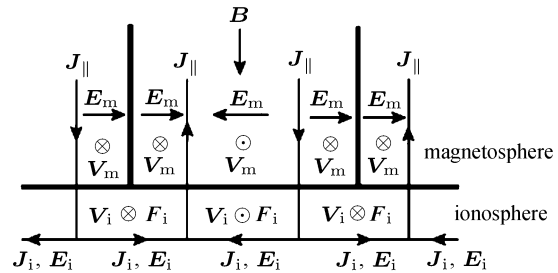


Figure 17 A dawn-dusk cut of northern-hemisphere ionosphere-magnetosphere interface viewed from the sun (Song *et al.*, 2000). The magnetosphere (ionosphere) is above (below) the thick horizontal line. The magnetic field points downward. The noon-midnight meridian is at the middle of the figure. The footprints of the boundary between the outer magnetosphere and LLBL/tail are indicated by the two thick vertical lines. The middle (outer) two field-aligned current J_{\parallel} are the NBZ (Region 1) currents. Subscripts m and i denote quantities in the magnetosphere and ionosphere, respectively. V , E , and F are the velocity, electric field, and Ampere force, respectively. Note that without the ionospheric coupling, the magnetospheric convection velocities on the two sides of a thick vertical line have no relationship, but they become coupled with the ionospheric currents which flow beneath the magnetosphere-ionosphere boundary.

state ionosphere, the $J \times \mathbf{B}$ force is balanced by the collisional force which is in the direction of the plasma flow (*e.g.*, Song *et al.*, 2005). The electric field is self-consistently produced in and not “penetrated” into the outer magnetosphere.

The plasmasphere is assumed to be, as in conventional models, controlled by the corotation and is not treated in detail.

With small variations, the model can be applied to the situations when IMF has an x -component or when the Earth’s dipole is tilted in the x - z plane. In these two cases, reconnection on the same IMF line takes place at the two cusps with a time difference. (At a given time, reconnection in two hemispheres occurs on two different IMF lines.) There are some observational differences from the simple case because during this time interval, the field line reconnected on one end is an open field. In other words, there is a small region of open field lines in each of the cusps.

Below we discuss briefly the relationship of the model with observations, another important aspect of global modeling: how to link a model to observations.

In this model the magnetosphere is closed except at the two cusps where reconnection takes place. The function of reconnection is to disconnect a portion of a closed field line on the nightside and at the same time to connect the left-over two ends with an IMF line forming a closed field line on the dayside. Note that this model applies to only steady states and is consistent with most simulation results. As we know, steady state magnetospheric convection takes some time to establish. Based on simulation results and an order analysis, it takes more than an hour to completely close the magnetosphere. Therefore a prolonged northward IMF is required before a closed magnetosphere can be observed. There have been observations on possible closed magnetosphere for strongly northward IMF (Fairfield, 1993; Fairfield *et al.*, 1996).

We should point out a significant difference between the last dayside closed field line and the stagnation streamline using MHD simulation diagnostics for northward IMF. When tracing the dayside field lines, one finds that the “magnetopause”, defined as the last closed field line, is located in point A in Figure 16. When tracing the solar wind streamlines, the “magnetopause”, defined as the stagnation point of the solar wind flow, is located at point B . Obser-

vationally, using the magnetometer data to identify the magnetopause, one finds point A and using the plasma data to identify the magnetopause, one finds point B . This difference was first pointed out by Song *et al.* (1990). Physically, the stagnation region of the magnetosheath flow, in steady state, is not at the magnetopause but at the inner edge of the LLBL. Therefore, in steady state, a stagnation point does not form at the magnetopause because plasma continuously flows across the magnetopause as discussed in Subsection 3.1. As the flow diverges from the equatorial local noon a stagnation line (Sonnerup, 1974) forms.

A stagnant region is expected to exist on the night side as well because a flow bifurcation is expected in this region. At point b in Figure 16(b), the flow is earthward (tailward) on the Earth (tail) side of the region. The distance of this region depends on how long the IMF has been northward. A long time after a northward turning, this region can be as close as $20\text{--}30 R_e$ from the Earth according to simulation results (Song *et al.*, 1999). Nevertheless, it may be as far as $100 R_e$ before the steady state is established. The plasma properties in this stagnant region depend on which side of the topological boundary that an observation is made and also on the most recent motion of the topological boundary. For example, on the tail side of point b in Figure 16, an observer will see high-density low temperature particles of solar wind origin if point b has just recently moved toward the observer. In the opposite situation, if point b has just recently moved earthward passing by the observer, the observer may see a nearly empty region. In a recent case study, Huang *et al.* (2002) showed evidence for such a bifurcation region. We believe that some of observations referred to as cold-dense plasma sheet are very likely related to this region (Fujimoto *et al.*, 1998; Phan *et al.*, 2000).

The outer magnetosphere consists of particles of magnetospheric origin with lower density and higher temperature. It convects in the same sense as the viscous cells. According to our global modeling principles there is no viscosity needed to drive such convection although it helps.

Although the magnetosphere is closed, the polar cap sees precipitation of solar wind particles as the captured solar wind flux tubes continuously lose their content. The precipitation may be related to

the polar rain which of solar wind origin has been interpreted as evidence for open field. The latter interpretation is not exclusive. This also shows an example of observational diagnostics needing to be carefully interpreted, especially for northward IMF. Latitudes lower than the polar cap see precipitation of magnetospheric origin.

In a dynamic process, northward IMF turning results in brightening of a narrow arc in the ionosphere centered near local noon and shifted with B_y . The arc propagates to lower latitudes and weakens before merging into the diffused aurora that is located at the boundary of the polar cap. Observations have shown such processes (Milan *et al.*, 2001). Variations in the IMF and hence in the reconnection rate result in wavy motion of the inner edge of the LLBL. Multiple transient reconnection episodes can form multiple distinction sublayers within the LLBL (Song and Russell, 1992).

One of the very interesting features in Figure 16(b) is the shaded region in the tail. It marks the region in transition of its topological status. Reconnection at the cusps has just disconnected this portion of magnetospheric flux tubes. If the magnetosphere is defined as the region with magnetic connection to the earth, this shaded region would be excluded. Therefore, there appears a dent in the night-side magnetosphere that has been shown clearly by Guzdar *et al.* (2001). On the dayside, on the other hand, the newly captured flux tube (as shown in Figure 12(b)) should, strictly speaking, be magnetospheric if using the same definition. However, in most of in-situ observations on the dayside, the magnetosphere is defined relative to the magnetopause current and not the topology. Therefore, this region may be classified as the magnetosheath. However, electron data may show some magnetospheric features (Onsager *et al.*, 2001).

3.3 Discussion

Computer simulations have become a significant tool for global modeling. However, sometimes simulations may not describe the intended processes although field line and streamline tracing creates continuous seamless colorful images. The knowledge of global modeling can help to identify the problem in simulations. Below we discuss two examples for flawed simulation results or interpretations although to identify the causes of the errors is beyond the scope of this

review. Nevertheless, it is understandable that not every simulationist is willing to share every technical detail of the simulation. We can only spot the inconsistencies. This is why to learn the principles of global modeling is so important for computer simulationists.

One example is the simulation for steady state due northward IMF with a reconnection region in the tail in addition to the two reconnection sites in the cusps, as discussed in Subsection 3.1 and sketched in Figure 18. Note that this result was presented as a steady state; namely, the simulation had run for a long time and the results did not change. First, we should state that this topology can occur during the transition period after the IMF turns from southward to northward. Before the northward IMF arrives, the magnetotail field lines are open beyond the tail reconnection region and they move toward the equator. When the northward IMF arrives, cusp reconnection takes place and starts forming closed field lines on the dayside. In order for reconnection to continue, a portion of the lobe magnetic field (on the nightside) starts moving toward the cusp reconnection regions. The ionospheric footprints of the field lines convect poleward and sunward. This motion in the lobes reduces the driving force for tail reconnection. One may expect that at a certain point, reconnection in the tail will have to cease. Therefore, the simulation result of steady state northward IMF with tail reconnection should be very suspicious. If one followed the princi-

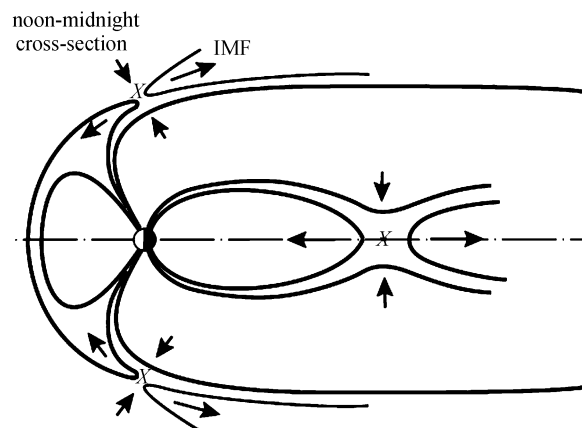


Figure 18 A magnetosphere for northward IMF with 3 reconnection sites. Solid lines indicate the magnetic field and the arrowheads indicate the direction of the flow. Reconnection sites are indicated by X.

ples discussed above, he/she would have difficulty to complete a full cycle of convection because the field lines in the noon-midnight meridian plane at mid-latitudes all move toward lower latitudes. No steady state could be achieved except if they move away from the Earth (to higher latitudes) in the terminators. However, one has to note that they are closed field lines and cannot be the ones that participate in reconnection either in the cusps or in the tail. If looked at the system's input and output, one would find that one IMF line comes into the system and 3 disconnected field lines are produced! This cannot be a steady state. Or, the three disconnected field lines connect into a single field line back to the solar wind. In this case, the single line will have to cross the tail open lines, a failure in complying with the principles of global modeling. Furthermore, and after all, the function of both cusp reconnection and tail reconnection is to connect two open field lines and produce a closed field line. With a limited number of open field lines produced during the previous southward IMF condition, sooner or later all field lines would become closed in order to reach the final steady state. A peculiar situation for this simulation result is that no ionospheric convection was shown.

An example of simulation that could lead to unphysical interpretations is that of Watanabe *et al.* (2005). This MHD simulation, using the same code as that of Song *et al.* (1999), dealt with a tilted Earth dipole field. In principle, as discussed above, the global model under this condition should be a variation of that described in Subsection 3.2. The simulation showed that because of the dipole tilt, reconnection at the two cusps does not take place on the same IMF at a given time or reconnection of the same IMF line take places at different times at the two cusps. An IMF line reconnects first to the hemisphere tilted toward the sun in one cusp and later with the one away from the Sun. In each polar ionosphere there is a region of open field lines. A peculiar feature occurs in this simulation when one traces the field lines from one hemisphere to the other. If starting with the field lines just inside the open-closed boundary, or the last-closed field lines, in one hemisphere which border a large polar cap region, one finds that these field lines converge to a very small region in the

other hemisphere. The same is true if starting from the other hemisphere. The last-closed field lines bordering a large polar cap region converge to a small region in this hemisphere. We now recall that as discussed in Subsection 2.2, if the magnetosphere and hence the ionosphere convects, unless the last-closed field lines are actually on the same streamline, the potential difference in the large area in one hemisphere would map to nearly a single point in the other hemisphere, resulting in an extremely large electric field at the converging point. The ionospheric convection velocity at this point would be extremely large but no such enhanced flow appears in the corresponding simulation figures. If indeed that there is no significant ionospheric flow near the converging point, when mapping the potential of this point back to the large area of the polar cap in the other hemisphere, there would be nearly no ionospheric convection. Therefore, this result is most likely due to the uncertainty in the field line tracing. Furthermore, as the field lines spread from a single point in each hemisphere to cover a large region in the other hemisphere, the field lines started from the two single points would have to intersect. This violates the principles we outlined in Subsection 2.2. One may attempt to attribute the violation to reconnection (Watanabe, private communication, 2009). In this case, for example, two nearly parallel field lines would reconnect at a place where their streamlines intersect. This situation would be a direct challenge to the validity of the field line tracing methodology.

4 Conclusions

We have outlined the principles of global modeling. These principles are not well documented previously in literature although widely used or abused in studies. With more and more results from global simulations, the importance of knowing these principles becomes increasingly crucial. We have provided an example of application of these principles and two counter examples. We have pointed out several common mistakes that some times appear in literature and frequently appear in discussions.

On the research front, although the global models for both due southward IMF and due northward

IMF have been proposed, there exists no global model for northward IMF with a B_y component that fully complies with the principles of global modeling outlined in this article. We strongly encourage the readers to attack this important but difficult problem.

References

- Axford W I, Hines C O. 1961. A unifying theory of high-latitude geophysical phenomena and geomagnetic storms [J]. *Can. J. Phys.*, **39**:1433
- Axford W I. 1963. Viscous interaction between the solar wind and the earth's magnetosphere [J]. *Planet. Space Sci.*, **12**:45
- Bartels J. 1932. Terrestrial-magnetic activity and its relations to solar phenomena [J]. *Terr. Magn. Atmosph. Ele.*, **37**, 1
- Bargatze L F, Ogine T R, McPherron L, Walker R J. 1999. Solar wind magnetic field control of magnetospheric response delay and expansion phase onset timing [J]. *J. Geophys. Res.*, **104**:14583
- Burch J L, Saffelos N A, Gurnett D A. 1992. Craven J D, Frank L A. The quiet time polar cap: DE 1 observations and conceptual model [J]. *J. Geophys. Res.*, **97**:A12, doi:10.1029/92JA01537
- Chapman S, Ferraro V C A. 1931. A new theory of magnetic storms [J]. *Terr. Mag.*, **36**:171
- Chandler M O, Fuselier S A, Lockwood M, Moore T E. 1999. Evidence of component merging equatorward of the cusp [J]. *J. Geophys. Res.*, **104**:22623
- Crooker N U. 1992. Reverse convection [J]. *J. Geophys. Res.*, **97**:19363
- Dungey J W. 1950. Some Researches in Cosmic Magnetism [D]. Cambridge: Cambridge University
- Dungey J W. 1961. Interplanetary magnetic field and the auroral zones [J]. *Phys. Rev. Lett.*, **6**:47
- Dungey J W. 1963. The structure of exosphere or adventures in velocity space [G]//Geophysics The Earth's Environment, DeWitt C, *et al* ed. New York: Gordon and Breach. 503
- Dungey J W. 1995. Origins of the concept of reconnection and its application to the magnetopause: A historical view [G]//Physics and The Magnetopause. Song P, *et al* ed. Geophys. Monograph, Vol. 90, 17
- Treumann R A, LaBelle J, Bauer T M. 1995. Diffusion processes: An observational perspective [G]//Physics and The Magnetopause. Song P *et al* ed., Geophys. Monograph, **90**:331
- Eastman T E. 1979. The Plasma Boundary Layer and Magnetopause Layer of the Earth's Magnetosphere [D]. Thesis: University Alaska
- Fairfield D H. 1993. Solar wind control of the distant magnetotail [J]. *J. Geophys. Res.*, **98**:21265
- Fairfield D H, Lepping R P, Frank L A, Ackerson K L, Paterson W R, Kokubun S, Tamamoto T, Tsuruda K, Nakamura M. 1996. Geotail observations of an unusual magnetotail under very northward IMF conditions [J]. *J. Geomagn. Geoelectr.*, **48**:473
- Fedder J A, Lyon J G. 1995. The Earth's magnetosphere is $165 R_e$ long: Self-consistent currents, convection, magnetospheric structure, and processes for northward interplanetary magnetic field [J]. *J. Geophys. Res.*, **100**:3623
- Fujimoto M, Terasawa T, Mukai T, Saito Y, Yamamoto T, Kokubun S. 1998. Plasma entry from the flanks of the near-earth magnetotail: Geotail observations [J]. *J. Geophys. Res.*, **103**:4391
- Gombosi T I, DeZeeuw D L, Groth C P T, Powell K G, Song P. 1998. The length of the magnetotail for northward IMF: Results of 3D MHD simulations [J]. *Phys. Space Plasmas*, **15**:121
- Guzdar P N, Shao X, Goodrich C C, Papadopoulos K, Wiltberger M J, Lyon J G. 2001. Three-dimensional MHD simulations of the steady state magnetosphere with northward interplanetary magnetic field [J]. *J. Geophys. Res.*, **106**:275
- Hines C O. 1963. The magnetopause: A new frontier [J]. *Science*, **141**:130
- Huang S S, Foster J C, Song P, Sofko G J, Frank L A, Paterson W R. 2002. Geotail observations of magnetospheric midtail during an extended period of strongly northward interplanetary magnetic field [J]. *Geophys. Res. Lett.*, **29**(4), 10.1029/2001GL014170
- Iijima T, Potemra T A. 1976. Field-aligned currents in the dayside cusp observed by triad [J]. *J. Geophys. Res.*, **81**, 34, doi:10.1029/JA081i034p05971
- Kan J R, Burke W J. 1985. A theoretical model of polar cap auroral arcs [J]. *J. Geophys. Res.*, **90**, A5, doi:10.1029/JA090iA05p04171
- Milan S E, Sato N, Ejiri M, Moen J. 2001. Auroral forms and the field-aligned current structure associated with field line resonances [J]. *J. Geophys. Res.*, **106**, A11, doi:10.1029/2001JA900077
- Newell P T, C I Meng. 1994. Ionospheric projections of magnetospheric regions under low and high solar wind pressure conditions [J]. *J. Geophys. Res.*, **99**, A1, doi:10.1029/93JA02273
- Ogino T, Walker R J. 1984. A magnetohydrodynamic simulation of the bifurcation of tail lobes during intervals with a northward interplanetary magnetic field [J]. *Geophys. Res. Lett.*, **11**:1018
- Ogino T, Walker R J, Ashour-Abdalla M. 1994. A global magnetohydrodynamic simulation of the response of the magnetosphere to a northward turning of the interplanetary magnetic field [J]. *J. Geophys. Res.*, **99**:11027
- Onsager T G, Scudder J D, Lockwood M, Russell C T. 2001. Reconnection at the high-latitude magnetopause during northward interplanetary magnetic field conditions [J]. *J. Geophys. Res.*, **106**:25467
- Parker E N. 1963. The solar-flare phenomenon and the theory of reconnection and annihilation of magnetic field [J]. *Astrophys. J.*, **8**(Supp.):177
- Phan T D, Lin R P, Fuselier S A, Fujimoto M. 2000. Wind observations of mixed magnetosheath-plasma sheet ion deep inside the magnetosphere [J]. *J. Geophys. Res.*, **105**:5497
- Petschek H E. 1964. Magnetic field annihilation [R]//AAS-NASA Symposium on Physics of Solar Flare. NASA Spec. Publ., **SP-50**, 425
- Raeder J. 1999. Modeling the magnetosphere for northward interplanetary magnetic field: Effects of electrical resistiv-

- ity [J]. *J. Geophys. Res.*, **104**:17357
- Raeder J, Walker R J, Ashour-Abdalla M. 1995. The structure of the distant geomagnetic tail during long periods of northward IMF [J]. *Geophys. Res. Lett.*, **22**:349
- Reiff P H, Burch J L. 1985. IMF By dependent plasma flow and Birkeland currents in the dayside magnetosphere, 2. A global model for northward and southward IMF [J]. *J. Geophys. Res.*, **90**, A2, doi:10.1029/JA090iA02p01595
- Russell C T. 1972. The configuration of the magnetosphere [G]//Critical Problems of Magnetospheric Physics. Dyer E R ed., Washington D C:Nat. Acad. of Sci., 1
- Siscoe G L, Lotko W, Sonnerup B U O. 1991. A high-latitude, low-latitude boundary layer model of the convection current system [J]. *J. Geophys. Res.*, **96**:3487
- Siscoe G L. 1987. The magnetospheric boundary [G]//Physics of Space Plasmas. Chang T, Crew G B, Jasperse J R ed., Cambridge: Scientific Publication Inc.
- Song P, Russell C T. 1992. A model of the formation of the low latitude boundary layer [J]. *J. Geophys. Res.*, **97**:1411
- Song P, Elphic R C, Russell C T, Gosling J T, Cattell C A. 1990. Structure and properties of the Subsolar magnetopause for Northward IMF:ISEE Observations [J]. *J. Geophys. Res.*, **95**:6375
- Song P, Russell C T, Fitzenreiter D J, Gosling J T, Thomsen M F, Mitchell D G, Fuselier S A, Parks G K, Anderson R R, Hubert D. 1993. Structure and properties of the subsolar magnetopause for northward IMF: Multiple instrument particle observations [J]. *J. Geophys. Res.*, **98**:11 319
- Song P, Russell C T, Gary S P. 1994. Identification of low-frequency fluctuations in the terrestrial magnetosheath [J]. *J. Geophys. Res.*, **99**:6011
- Song P, DeZeeuw D L, Gombosi T I, Groth C P T, Powell K G. 1999. A numerical study of solar wind-magnetosphere interaction for northward IMF [J]. *J. Geophys. Res.*, **104**:28 361
- Song P, Gombosi T I, DeZeeuw D L, Powell K G, Groth C P T. 2000. A model of solar wind-magnetosphere-ionosphere coupling for northward IMF [J]. *Planet. Space Sci.*, **48**:29
- Song P, Gombosi T I, Ridley A. 2001. Three-fluid Ohm's law [J]. *J. Geophys. Res.*, **106**:8149
- Song P, Vasyliūnas V M, Ma L. 2005. Solar wind-magnetosphere-ionosphere coupling: Neutral atmosphere effects on signal propagation [J]. *J. Geophys. Res.*, **110**, A0909309, doi:10.1029/2005JA011139
- Sonnerup B U O. 1974. The reconnecting magnetosphere [G]//Magnetospheric Physics. McCormac B M ed., Dordrecht Holland: D. Reidel Publ. Co. 23-33
- Sonnerup B U O. 1980a. Theory of the low-latitude boundary layer [J]. *J. Geophys. Res.*, **85**:2017
- Sonnerup B U O. 1980b. Transport mechanisms at the magnetopause [G]//Dynamics of the Magnetosphere. S I Aka-sofu ed., Hingham: D Reidel Publishing Co. Mass.77
- Sweet P A. 1958. The neutral point theory of solar flares [G]//Electromagnetic Phenomena in Cosmic Physics. Lehnert B ed., Cambridge: Cambridge University Press. 135
- Toffoletto F R, Siscoe G L. 2009. Solar-wind-magnetosphere coupling: an MHD perspective [G]//Heliophysics I: Plasma Physics of the Local Cosmos. Cambridge: Cambridge University Press
- Tonks L, Langmuir I. 1929. Oscillations in ionized gases [J]. *Phys. Rev.*, **33**:195
- Tu J, Song P, Reinisch B W. 2008. On the concept of penetration electric field [G]//Radio Sounding and Plasma Physics. AIP Conference Proceeding. **974**:81-85
- Usadi A, Kageyama A. 1993. Watanabe K, Sato T. A global simulation of the magnetosphere with a long tail: Southward and northward interplanetary magnetic field [J]. *J. Geophys. Res.*, **98**:7503
- Vasyliūnas V M. 1970. Mathematical models of magnetospheric convection and its coupling to the ionosphere [G]//Particles and Fields in the Magnetosphere. McCormack B M ed. D. Reidel Publishing Co., DordrechtHolland. 60-71
- Vasyliūnas V M. 1972. Nonuniqueness of magnetic field line motion [J]. *J. Geophys. Res.*, **77**:6271
- Vasyliūnas V M. 1975. Theoretical models of magnetic field line merging [J]. *Rev. Geophys. Space Phys.*, **13**:303
- Vasyliūnas V M. 1984. Steady state aspects of magnetic field line merging [G]//Magnetic Reconnection in Space and Laboratory Plasma. Hones E W Jr. ed., Geophys. Monograph, **30**:25
- Vasyliūnas V M. 2001. Electric field and plasma flow: What drives what [J]. *Geophys. Res. Lett.*, **28**:2177-2180
- Vasyliūnas V M. 2005a. Time evolution of electric fields and currents and the generalized Ohm's law [J]. *Ann. Geophys.*, **23**:1347-1354
- Vasyliūnas V M. 2005b. Relation between magnetic fields and electric currents in plasmas [J]. *Ann. Geophys.*, **23**:2589-2597
- Vasyliūnas V M. 2007. The mechanical advantage of the magnetosphere: Solar-wind-related forces in the magnetosphere-ionosphere-Earth system [J]. *Ann. Geophys.*, **25**:255
- Vasyliūnas V M, Song P. 2005. Meaning of ionospheric Joule heating [J]. *J. Geophys. Res.*, **110**, A02301, doi:10.1029/2004JA010615
- Watanabe M, Kabin K, Sofko G J, Rankin R, Gombosi T I, Ridley A J, Clauer C R. 2005. Internal reconnection for northward interplanetary magnetic field [J]. *J. Geophys. Res.*, **110**, A6, doi:10.1029/2004JA010832
- Wolf R A. 1970. Effects of ionospheric conductivity on convective flow of plasma in the magnetosphere [J]. *J. Geophys. Res.*, **75**:4677-4698